A Critical Review of the Semi-Physical Modeling of Soil-Water Characteristic Curve

Hongyu Tu*,1,2, Sai Vanapalli[1]

[1]*Department of Civil Engineering, University of Ottawa, Ottawa, Canada*
[2]*Keller North America, Toronto, Canada*

**Corresponding author's email:* htu104@uottawa.ca

Abstract: A unified framework for estimating the Soil-Water Characteristic Curve (SWCC) for the entire suction range (i.e., 0 to 1,000,000 kPa) by extending semi-physical approach is promising. This paper provides a critical review of various semi-physical models from the literature for predicting the SWCC. The focus of the review in this paper is directed to highlight the models built based on strong relationships between the soil grain size properties and their pore-size distribution – a key factor that influences the shape of the SWCC. The SWCC models are classified into two categories; namely, capillary tube bundle models and pore-scale models, based on the assumptions and limitations inherited in each approach for representing soil porosity. In addition, a succinct discussion is provided for explaining water retention in soils associated both with the capillary and adsorption mechanisms over the complete range of suction.

Introduction

The hydro-mechanical properties of unsaturated soils vary with respect to suction in a nonlinear fashion [1], [2], [3], [4]. Therefore, it is important to understand the Soil-Water Characteristic Curve (SWCC), which is widely used as a pillar stone for predicting and interpreting the hydro-mechanical behaviors of unsaturated soils. The shape of a SWCC is strongly dependent on its pore-size distribution [5]. Many studies were devoted in the literature towards developing semi-physical models to construct a representative pore-size distribution (PoSD) and use it to predict the SWCC based on the grain-size properties along with information of other basic soil index properties [6], [7]. The semi-physical models usually involve numerical discretization and reassembling of the soil mass as two essential steps. Unless a controlling mechanism is introduced for the reassembling process, the resulting pore size distribution would only share the same shape and tendency as the probability distribution of the Grain Size Distribution Curve (GSDC), or in other words, the modality of the SWCC would only mirror the modality features of the GSDC. To alleviate this concern, Arya and Paris (AP) models [6], [7] proposed a scaling parameter to control the packing. The selection of the scaling parameter could be arbitrary or dependent on other parameters [8]. Several studies revealed a dual-, or even multi-porosity feature for many soils. Some studies have proposed the judgement criteria for the SWCC modality facilitating in the determination of model parameters based on regression techniques [9], [10]. However, these models introduce several model parameters and are validated using limited databases. The above discussed limitations encourage a unified framework for modeling the SWCC without presupposition of the SWCC modality. For this reason, the semi-physical modeling is promising in constructing a distinctive porosity (or porosities) for individual soils, rather than empirically correlating the conceptual SWCC equation parameters to other soil properties. There is a greater chance of success in the reliable prediction of the SWCC and can be extended as a tool in the reliable prediction of non-linear properties of unsaturated soils in geotechnical engineering practice applications using semi-physical models. The key objective of this paper is to provide a comprehensive review of the semi-physical models in the literature for predicting the SWCC.

Physical Phases of Pore-Water

In granular physics, the transitioning of the liquid within the granular media can be classified into five regimes, namely, i) saturated regime, ii) capillary regime, iii) funicular, iv) pendular regime, and v) dry regime [11]. Collectively, the capillary regime and funicular regime can be considered as the equivalent of boundary effective zone and transition zone, respectively; the combination of pendular regime and dry regime can be considered as the equivalent of zone of residual saturation. The description, dominating flow, pattern of liquid (water), and schematic diagram of water of all five regimes are summarized in Table 1.

Table 1: Five Phases of Pore-Water

Granular media regime	Saturated regime	Capillary regime	Funicular regime	Pendular regime	Dry regime
Dominating flow	Capillary flow				Film flow
Pattern of water	Water-filled pores		Water-filled pores and liquid bridges	Liquid bridges	Film water
Schematic diagram	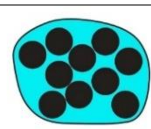		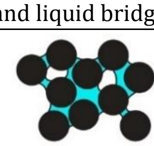	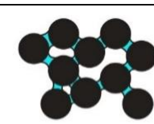	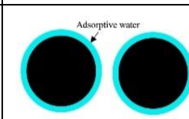
Stages of desaturation	Saturated Condition	Boundary Effect Zone	Transition Zone	Zone of Residual Saturation	

The capillary law dominates the regimes where either or both the liquid-filled pores, and the liquid bridges around the contact points exist. Upon drying, the liquid-filled pores become desaturated, and the pore water shrinks into liquid bridges spanning the adjacent grains. The desaturated spaces are often referred to as pore throats [12]. The capillary force that prevents the desaturation of the pore throat of a certain size is its corresponding snap-off suction [13], [14]. The snap-off suction corresponding to the air entry value will be controlled by the routing radius, namely the radius of the largest sphere that can pass through the porous medium [10]. Upon the development of pore throats, the pore water exists in the form of liquid bridges at the corners of the adjacent grains, which also is referred to as the toroidal meniscus water [15], [16]. Once the pore throats are fully developed, the capillary water only exist in the form of liquid bridges and the wet granular is at pendular regime, corresponding to the primary stage of the SWCC zone of residual saturation. Capillary flow would cease once all liquid bridges are completely desaturated. At this point, the residual water exists only in the form of adsorptive water (or water film) adhering to the surface of the grains, corresponding to the secondary stage of the SWCC zone of residual saturation [17], [18], [19].

Hypothesizes Used for Soil Porosity Assuming Packing of Idealized Spherical Particles

This review focuses on the packing of idealized spherical particles. The packing of soil particles typically requires hypotheses to be made on these areas: (1) the discretization of soil mass; (2) the assembly of particle packing.

While many numerical methods such as Discrete Element Method (DEM) can be used to artificially generate a population of randomly packed particles [14], [20], this paper focuses on reviewing the modeling processes associated with the discretization method that divides the GSDC into *n* fractions (domains) (see Figure 1a), each consisting of a group of unified soil particles of the median particle diameter [6], [7].

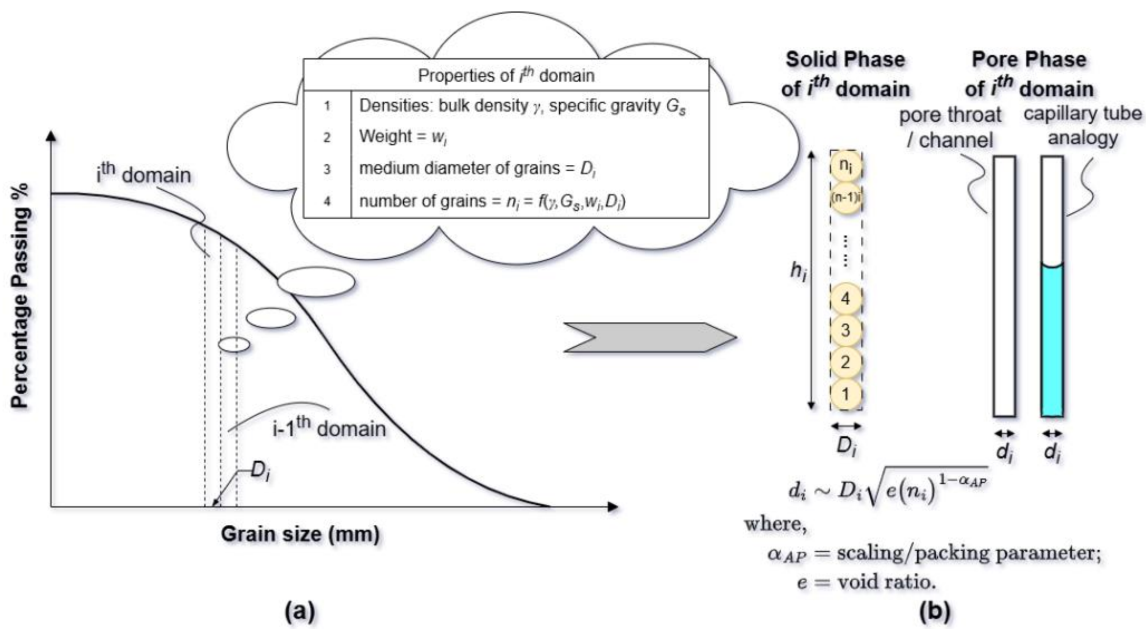

Figure 1: Physical Hypothesis Adopted by AP Model: (a) Discretization, (b) Re-assembling

Different physical hypothesises are made by different studies to assemble the particles together. These hypothesises can be summarized into two types, as follows:

Packing Method 1: the uniform particles of each domain are packed along a hypothetical linear path; the pore channel of each domain is assumed to be a capillary tube, the length of which is either the same as, or scaled from the hypothetical path followed by the arrangement of particles. This group of models is classified as capillary tube bundle models in this paper.

Packing Method 2: the uniform particles of each domain are packed in either 2D or 3D space; a population of pore spaces is generated from this process. A scaling parameter or technique is often introduced to harmonize the generated porosity with the apparent porosity measured from the physical tests. This group of models is classified as pore-scale models in this study.

Capillary Tube Bundle Models

Arya and Paris (1981) proposed the pioneering capillary tube bundle model (AP model). The water flow paths in a soil are treated as a bundle of capillary tubes and assume that sizes of soil particles are related to corresponding pore diameters of the capillary tubes. The capillary volume is a function of particle size, mass fraction of the particle size, and a scaling parameter which was initially treated as a constant [6] and later as a variable parameter for different particle sizes [7].

The physical hypothesis inherited in this model is illustrated in Figure 1. In each domain, all the sphere particles of a same diameter will be packed as one layer, along a linear path with length (h_i); the pore phase at each domain is assumed to be a cylindrical tube of the same length; the diameter of each capillary tube (d_i) can be calculated from the volume-mass relationship; and, most importantly, as with any idealized process, the generated porosity deviates from the actual condition, a calibration process is required by introducing a parameter [6], [7] to scale the tortuosity of the pore channels, or shape parameters to scale the effect of the actual shape of the particles and the pores [21].

The relation between the median diameter of particles and the diameter of the corresponding hypothetical pore throat / channel was expressed as Equation (1).

$$d_i = D_i\sqrt{e(n_i)^{1-\alpha_{AP}}} \quad (1)$$

where, the nomenclature refers to Figure 1b.

While the assumed physical process is simple and idealistic, a reliable estimation of the scaling parameter (α_{AP}) is crucial for the performance of the AP model. The original model and a subsequent revision recommended a constant value of = 1.38, and 0.938, respectively, for all soils. Some studies [22], [23] opined that instead of using a constant value, a variable α_{AP} leads to better SWCC estimation. Arya et al. [7] modified their original work providing three different options: (i) constant parameters corresponding to five representative soil textures (sand, sandy loam, loam, silt loam, and clay), (ii) variable parameter as a logistic growth curve of the logarithmized number of grains (log n_i), and (iii) linear equation of logarithmized median grain size, mass fraction (log w_i/R_i^3) and number of grains (log n_i). Antinoro et al. [24] found that the logistic growth equation allowed more accurate predictions compared to the linear equation for Sicilian soils ranging in soil texture from sand to clay. However, Huang et al. [25] could not identify significant improvement in the performance of the AP model by using a continuous function to estimate α_{AP} for all textural groups from the Loess Plateau, China.

The mathematical representation of the GSDC, and the number of the discrete domains are also critical for the performance of the AP or AP-derived models. Nasta et al. [26] and Liu et al. [27] used a same equation to statistically define both the GSDC and SWCC. Both studies found that prior separation of soil textural classes provide better scaling results, Liu et al. [27] optimized the α_{AP} as constant values corresponding to different soil textural classes. Nasta et al. [26] proposed that the α_{AP} parameter would typically be in the range between 1 and 1.2 for all soil textural classes investigated and further demonstrated that only 30 soil discrete domains were required for a reliable modeling of the SWCC.

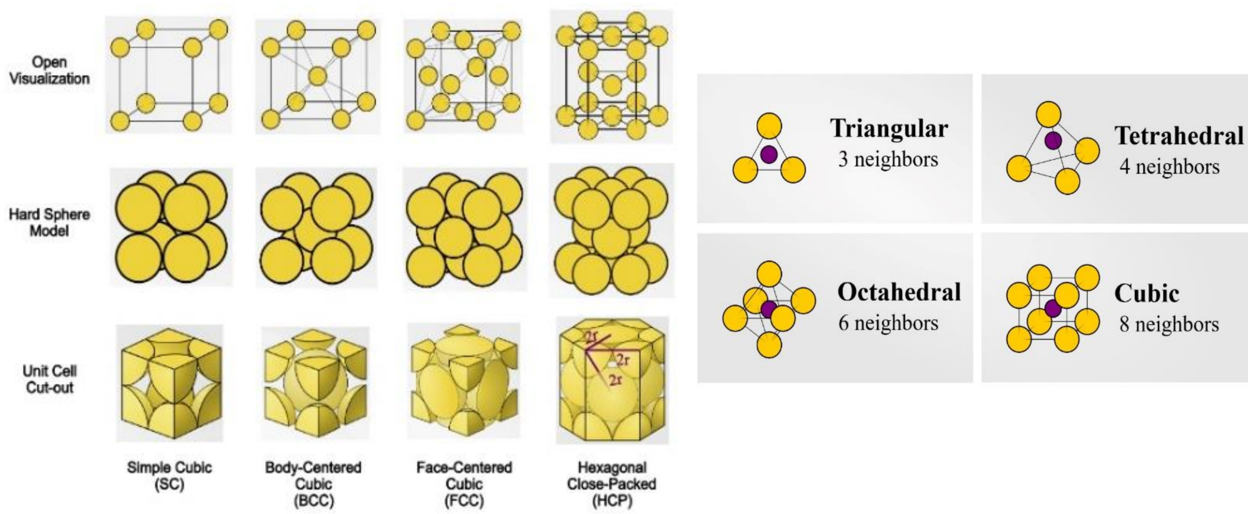

Figure 2: Four Typical Sphere Packings and Four Associated Interstitial Sites (from [32])

Pore-Scale Models

While the actual natural soil mass is randomly assembled polydisperse particles of non-spherical shape, to render the assembly requires fairly rigorous algorithm to execute the 'random' combination of particles from the entire population of particles of various of diameter, and complex hypothesises accompany with it. Therefore, most of the studies, that proposed pore space models, took the alternative approach by assembling a series of unit cells of monodisperse particle packing in either 2D or 3D space.

Among numerous of packing patterns, simple cubic (SC), body-centered cubic (BCC), face-centered cubic (FCC), and hexagonal close-packed (HCP), allows the monodisperse spherical particles to touch all the neighboring particles. As such, these packing patterns feature non-elongated interstitial voids and explicit unit cell properties. Therefore, they are often extended in different studies to construct the pore-scale modeling of SWCC. While some other packing patterns, such as simple rhombohedral (SR) and those in which spheres are not touching, featuring elongated or irregular interstitial voids, can be used to model the hydraulic hysteresis.

Pore-Throat

The suction at which snap-off occurs is known as the snap-off suction. The Young-Laplace equation (2) relates the snap-off suction to the surface tension, T_s and the radius r of the throat.

$$s = \frac{2T_s \cos\beta}{r} \tag{2}$$

where, s is the matric suction, β is the contact angle.

For the case of 2-D particles touching each other, the radius of the pore-throat can be determined based on trigonometry. For the case of kissing 3-D particles, the radius of the pore-throat is related to the radius of interstitial sites [12]. The radius of each type of interstitial site varies with respect to different packing structures (Figure 2), Table 2 provides a summary of the size factors of different interstitial sites corresponding to typical sphere packings.

Table 2: Diameter of Various Interstitial Sites Corresponding to Typical Sphere Packings

	Interstitial Site	
Packing Structure	**Type**	**Size ratio**
Simple cubic (SC)	Cubic	√3-1 ≈ 0.732
Body-centred cubic (BCC)	Tetrahedral	√5/√3-1 ≈ 0.291
	Octahedral	2/√3-1 ≈ 0.155
Face-centred cubic (FCC)	Tetrahedral	√6/2-1 ≈ 0.225
	Octahedral	√2-1 ≈ 0.414
Hexagonal close-packed (HCP)	Tetrahedral	√6/2-1 ≈ 0.225
	Octahedral	√2-1 ≈ 0.414

Note: size ratio is the ratio of the diameter of interstitial site to the diameter of the spherical particles

Toroidal meniscus water (liquid bridge)

A liquid bridge is formed when water is present at the contact points between particles in the pendular regime (Figure 3). Real soil particles have irregular shapes but idealizing them as spheres makes calculations easier [14]. For the case of two touching monodispersed spheres, the nodoid is the mathematically correct shape for the liquid-vapor interface of a pendular ring.

However, the nodoid shape is complex, making it difficult to calculate analytically. The study by Mayer and Stowe [28] concluded that the toroid model provides accurate results with negligible differences in pressure-volume relationships compared to the nodoid. As such, the toroid as a computationally simpler approximation of the meniscus is often adopted [14], [15].

The volume of the toroidal meniscus (V_{toroid}) is typically calculated considering an axial symmetry along lines joining the centers of two particles and symmetry relative to the plane of contact between the particles. The analytical solution of the meniscus volume of the simplified toroidal model was presented by Cao et al. [15] as Equation (3). The corresponding matric suction was expressed as Equation (4).

$$V_{\text{toroid}} = 2\left\{\begin{array}{c} 2\pi R^2 \sin\gamma \cdot (1-\cos\gamma) - \dfrac{\pi}{6}\cdot R(1-\cos\gamma)\left[3(R\sin\gamma)^2 + R^2(1-\cos\gamma)^2\right] \\ +\dfrac{2\pi}{3}[R(1-\cos\gamma)]^{3/2} \\ -\pi\left(R\sin\gamma + \dfrac{R(1-\cos\gamma)}{\cos(\beta+\gamma)}\cos(90^\circ-\gamma-\beta)\right)\left[\dfrac{R(1-\cos\gamma)}{\cos(\beta+\gamma)}\right]^2 \\ \times\left[\dfrac{\pi}{2}-(\beta+\gamma)-\sin(\beta+\gamma)\cos(\beta+\gamma)\right] \end{array}\right\} \tag{3}$$

$$s = T_s\frac{\cos(\beta+\gamma)}{R(1-\cos\gamma)} \tag{4}$$

where, γ is the fill angle of meniscus water.

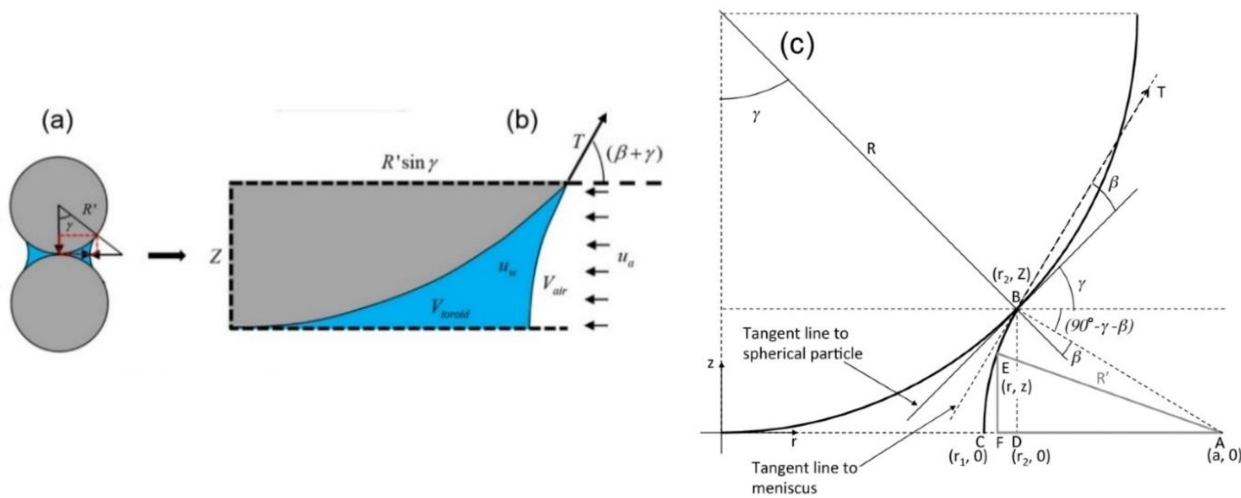

Figure 3: Illustration of Meniscus Water and Toroidal Model (after [15])

Film water

Further recessed pore water will be held as thin films on soil particle surfaces by the adsorptive force. Capillary condensation as the reversed process occurs where adsorbed water films become thick enough to form liquid bridges [17].

The suction in soil is comprised of both the capillary and adsorptive components. A theoretical concept was initially proposed by Or and Tuller [19] suggesting the SWCC can be broken down into the capillary contribution and the adsorptive contribution, as illustrated in Figure 4. This theoretical concept has since been succeeded by many studies, which formulated the capillarity and adsorption as separate terms (S^{cap}, and S^{ads}), as equation (5).

$$S = S^{\text{cap}} + S^{\text{ads}} \tag{5}$$

Or and Tuller [19] proposed an upscaling model for liquid retention and interfacial area statistically links pore-scale liquid behavior to sample-scale properties in variably saturated porous media. Unlike the sphere packing, this model uses a unit cell consisting of an angular central pore for capillary processes and slit-shaped spaces for adsorption. The distribution of central pore lengths is represented by a gamma distribution, facilitating closed-form expressions for liquid retention and interfacial area, and the adsorption curve. Zhou et al. [17] and Qian et al. [18] incorporated this concept for fine-grained soils, and proposed equation (6) to conceptually represent the adsorption curve. Although presenting the schematics using spherical particles (Figure 4), both studies shared the same theoretical concepts originated by Or and Tuller [19] based on unit cells of an arbitrary shape, rather than spherical packing.

$$S^{\text{ads}} = \beta^{\text{ads}}\left(1 - \frac{ln\, s}{ln\, s_d}\right) f \qquad (6)$$

where, β^{ads} is a fitting parameter [18], or can be expressed as (θ_0/θ_s) [17], f is the possibility of capillary condensation expressed as (ln s/ ln s_d) [18] or (1-S^{cap}) [17], s_d is the maximum suction under oven-dry conditions.

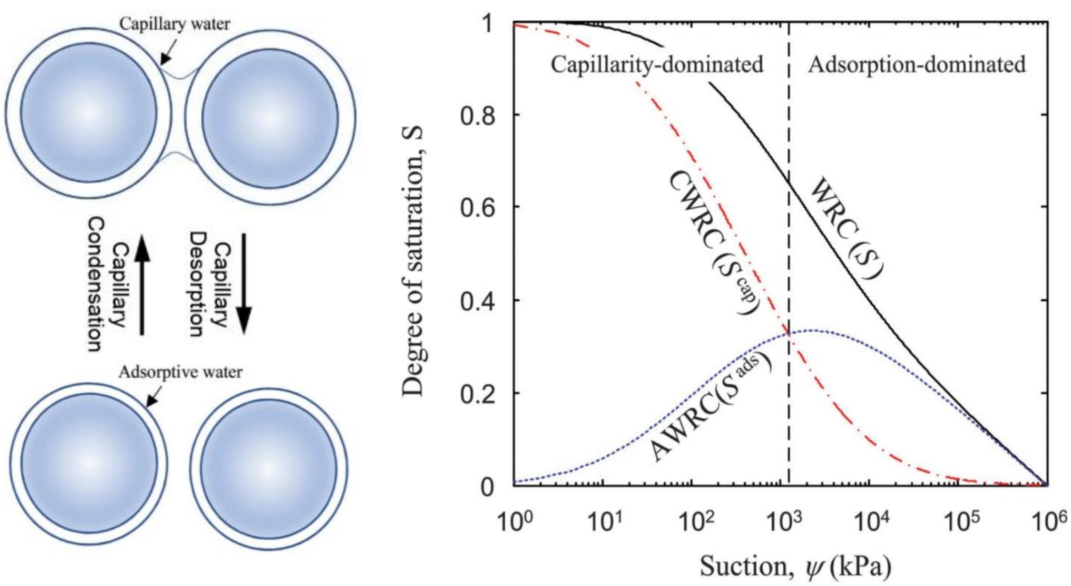

Figure 4: Schematic diagram for soil-water characteristic curve considering both capillarity and adsorption (after [17], [18])

Dolinar [29] proposed a different semi-empirical model based on the relationship between soil suction and specific surface area (A_s), considering the water content, the thickness of adsorbed water layer (t), and more importantly, the concept of a double-porosity model for pore-space geometry. It assumes that water in clay aggregates is adsorbed and that van der Waals forces dominate the adsorption mechanism, while the water in the macropores is dominated by capillary forces. At equilibrium, the water in the clay aggregates and macropores must be in the same energy state (i.e., $s = s_{\text{cap}} = s_{\text{ads}}$), or equivalently. The conceptual model considering both the capillary and adsorption contribution was formulated as equation (7).

$$\begin{cases} s = s_{\text{ads}} = s_{\text{cap}} \\ s_{\text{ads}} = \dfrac{A_{svi}}{6 \cdot \pi \cdot t^3} \\ w_{\text{ads}} = (w - w_p) = t \cdot A_S \cdot \rho_w \\ w_p = p \cdot 69.389 \cdot t^{0.288} \end{cases} \Rightarrow \quad w = 0.147 \cdot s^{-0.333} \cdot A_S + p \cdot 0.747 \cdot s^{-0.096} \tag{7}$$

where, w is the gravimetric water content corresponding to matric suction s, w_p is the gravimetric water content in the macropores corresponding to matric suction due to the capillary, w_{ads} is the gravimetric water content corresponding to matric suction due to the adsorption in the aggregate, p is the content (%) of clay minerals in the soil divided by 100 ($0 < p \leq 1$), A_{svi} is the Hamaker constant for solid-vapor interactions through the intervening liquid, A_S is the external specific surface area (m^2/g).

The conceptual model equations reviewed in this study, and many more that were proposed in the literature incorporating the contribution of adsorption phase, such as MK model [30], can be used to project the SWCC curve with the full suction range. However, the curve projection in the high suction range is sensitive to the model fitting parameters. Their use is better suited when the measurements of matric suction in the high suction range are available. Such measurements, however, are challenging.

Several empirical methods exist for estimating the SWCC at the high suction range, which is particularly relevant to the adsorption zone. For example, Jensen et al. [31] proposed to estimate the water content θ_{PF6} corresponding to matric suction pF 6 and further interpolate the volumetric water contents θ_{PF} at other four prescribed matric suction values pF 5.2, 5.5, 5.7, 6.3.

$$\begin{cases} \theta_{pF} = \dfrac{\theta_{pF6}(6.9 - pF)}{6.9 - 6} \qquad (pF = 5.2, 5.5, 5.7, 6.3) \\ \theta_{pF6} = 0.08(\text{C} + 2\ \text{OM} + 0.15\ \text{Si})\rho_b \end{cases} \tag{8}$$

where, C is clay fraction, Si is silt fraction, OM is organic matter, ρ_b is bulk density.

Summary

For better understanding the SWCC behavior over the entire range of suction, it is critical to understand the physical phases of the pore-water through all five regimes: saturated, capillary, funicular, pendular, and dry (adsorption). It is possible to estimate the Soil-Water Characteristic Curve (SWCC) for the entire suction range (i.e., 0 to 1,000,000 kPa) by extending semi-physical approach. The semi-physical models use hypothetical discretization and reassembling of the soil mass, resulting in a pore size distribution. Packing of idealized spherical particles can be achieved using methods such as capillary tube bundle models and pore-scale models that provide analytical solutions for the pore-water volume and matric suction through different phases. These models help to understand phenomena like snap-off suction at pore throats, the formation of toroidal meniscus water (liquid bridges) in the pendular regime, and the presence of film water on soil particle surfaces. A unified framework using a semi-physical approach for estimating the SWCC for the entire suction range, free of presupposition of the SWCC modality, is a promising approach to explore, and will be reported in a separate study.

References

[1] S. K. Vanapalli, D. G. Fredlund, D. E. Pufahl, and A. W. Clifton. Model for the prediction of shear strength with respect to soil suction. *Canadian Geotechnical Journal*, 33(3):379–392, 1996.

[2] D. G. Fredlund, N. R. Morgenstern, and R. A. Widger. The shear strength of unsaturated soils. *Canadian Geotechnical Journal*, 15(3): 313–321, 1978.

[3] D. Sheng, A. Zhou, and D. G. Fredlund. Shear Strength Criteria for Unsaturated Soils. *Geotechnical and Geological Engineering*, 29(2):145–159, 2011.

[4] S. L. Houston, N. Perez-Garcia, and W. N. Houston. Shear Strength and Shear-Induced Volume Change Behavior of Unsaturated Soils from a Triaxial Test Program. *Journal of Geotechnical and Geoenvironmental Engineering*, 134(11): 1619–1632, 2008.

[5] P. H. Simms and E. K. Yanful. Estimation of Soil–Water Characteristic Curve of Clayey Till Using Measured Pore-Size Distributions. *Journal of Environmental Engineering*, 130(8):847–854, 2004.

[6] L. M. Arya and J. F. Paris. A Physicoempirical Model to Predict the Soil Moisture Characteristic from Particle-Size Distribution and Bulk Density Data. *Soil Science Society of America Journal*, 45(6):1023–1030, 1981.

[7] L. M. Arya, F. J. Leij, M. Th. van Genuchten, and P. J. Shouse. Scaling Parameter to Predict the Soil Water Characteristic from Particle-Size Distribution Data. *Soil Science Society of America Journal*, 63(3):510–519, 1999.

[8] C. Wang, S. Li, X. He, Q. Chen, H. Zhang, and X. Liu. Improved prediction of water retention characteristic based on soil gradation and clay fraction. Geoderma, 404, p. 115293, Dec. 2021, doi: 10.1016/j.geoderma.2021.115293.

[9] A. Satyanaga, H. Rahardjo, E.-C. Leong, and J.-Y. Wang. Water characteristic curve of soil with bimodal grain-size distribution. *Comput Geotech*, 48:51–61, 2013.

[10] X. Li, J. H. Li, and L. M. Zhang. Predicting bimodal soil–water characteristic curves and permeability functions using physically based parameters. *Comput Geotech*, 57:85–96, 2014.

[11] N. Mitarai and F. Nori. Wet granular materials. *Adv Phys*, 55(1–2):1–45, 2006.

[12] R. D. Alves, G. de F. N. Gitirana Jr., and S. K. Vanapalli. Advances in the modeling of the soil–water characteristic curve using pore-scale analysis. *Comput Geotech*, 127(103766):1-12, 2020.

[13] W. J. Stroud, J. E. Curry, and J. H. Cushman. Capillary Condensation and Snap-off in Nanoscale Contacts. *Langmuir*, 17(3):688–698, 2001.

[14] B. Bate, S. Nie, Z. Chen, F. Zhang, and Y. Chen. Construction of soil–water characteristic curve of granular materials with toroidal model and artificially generated packings. *Acta Geotech*, 16(6):1949–1960, 2021.

[15] J. Cao, J. Jung, X. Song, and B. Bate. On the soil water characteristic curves of poorly graded granular materials in aqueous polymer solutions. *Acta Geotech*, 13(1):103–116, 2018.

[16] N. Lu, J. Lechman, and K. T. Miller. Experimental Verification of Capillary Force and Water Retention between Uneven-Sized Spheres. *J Eng Mech*, 134(5):385–395, 2008.

[17] A. Zhou, R. Huang, and D. Sheng. Capillary water retention curve and shear strength of unsaturated soils. *Canadian Geotechnical Journal*, 53(6):974–987, 2016.

[18] J. Qian, Z. Lin, and Z. Shi. Soil-water retention curve model for fine-grained soils accounting for void ratio–dependent capillarity. *Canadian Geotechnical Journal*, 59(4):498–509, 2022.

[19] D. Or and M. Tuller. Liquid retention and interfacial area in variably saturated porous media: Upscaling from single-pore to sample-scale model. *Water Resour Res*, 35(12):3591–3605, 1999.

[20] M. Farahnak, R. Wan, and M. Pouragha. Exploring the tensorial nature of capillary stress and the constitutive role of contact stress in wet granular materials. *Comput Geotech*, 173(106492):1–14, 2024.

[21] A. R. Russell. How water retention in fractal soils depends on particle and pore sizes, shapes, volumes and surface areas. *Geotechnique*, 64(5):379–390, 2014.

[22] K. Van Looy et al. Pedotransfer Functions in Earth System Science: Challenges and Perspectives. *Reviews of Geophysics*, 55(4):1199–1256, 2017.

[23] C. M. P. Vaz et al. Validation of the Arya and Paris Water Retention Model for Brazilian Soils. *Soil Science Society of America Journal*, 69(3):577–583, 2005.

[24] C. Antinoro, V. Bagarello, V. Ferro, G. Giordano, and M. Iovino. A simplified approach to estimate water retention for Sicilian soils by the Arya–Paris model. *Geoderma*, 213:226–234, 2014.

[25] M. Huang, D. G. Fredlund, and M. D. Fredlund. Comparison of Measured and PTF Predictions of SWCCs for Loess Soils in China. *Geotechnical and Geological Engineering*, 28(2):105–117, 2010.

[26] P. Nasta, T. Kamai, G. B. Chirico, J. W. Hopmans, and N. Romano. Scaling soil water retention functions using particle-size distribution. *J Hydrol*, 374(3-4):223–234, 2009.

[27] S. Y. Liu, N. Yasufuku, Q. Liu, and J. Yu. Prediction of soil water characteristic curve using physically based scaling technique. Lowland Technology International, 15(1):10–20, 2013.

[28] R. P. Mayer and R. A. Stowe. Nodoids and toroids: comparison of two geometries for the meniscus profile of a wetting liquid between two touching isolated spheres and extensions to the model of a collection of packed spheres. *J Colloid Interface Sci*, 285(2):781–788, 2005.

[29] B. Dolinar. Prediction of the soil-water characteristic curve based on the specific surface area of fine-grained soils. *Bulletin of Engineering Geology and the Environment*, 74(3):697–703, 2015.

[30] M. Aubertin, M. Mbonimpa, B. Bussière, and R. P. Chapuis. A model to predict the water retention curve from basic geotechnical properties. *Canadian Geotechnical Journal*, 40(6):1104–1122, 2003.

[31] D. K. Jensen, M. Tuller, L. W. de Jonge, E. Arthur, and P. Moldrup. A New Two-Stage Approach to predicting the soil water characteristic from saturation to oven-dryness. *J Hydrol*, 521:498–507, 2015.

[32] https://msestudent.com/. Accessed on Jan 10, 2025.